A&A 460, 953–958 (2006)
DOI: 10.1051/0004-6361:20066033

Astronomy & Astrophysics

Collisional excitation of monodeuterated ammonia NH_2D by helium

L. Machin and E. Roueff

Laboratoire Univers et Théories and UMR 8102, Observatoire de Paris-Meudon, 5 place Jules Janssen, 92195 Meudon, France
e-mail: [leandre.machin;evelyne.roueff]@obspm.fr

Received 13 July 2006 / Accepted 21 August 2006

ABSTRACT

Context. Observations of deuterated molecules are useful probes of the physical and chemical conditions in star-forming regions. However their detailed interpretation is hampered by the lack of knowledge of the corresponding collisional rate coefficients.
Aims. We extend our previous study of ammonia collisional excitation by helium to monodeuterated ammonia NH_2D, which has been found to be abundant in a variety of environments.
Methods. We introduce the principal isotopic effects in the collisional equations by calculating the relevant angular dependence of the intermolecular potential energy surface.
Results. Cross sections are calculated in the coupled states approximation, and collisional rate coefficients are given from 5 to 100 K, a range of temperatures that is relevant in the interstellar medium.
Conclusions. These results allow to include justifiable collisional excitation rate coefficients of NH_2D by He in the analysis of the emitted radiation for the first time

Key words. ISM: general – ISM: molecules – molecular data – molecular processes – scattering

1. Introduction

Ammonia NH_3 is the first polyatomic molecule observed in the interstellar medium via centimetric transitions arising within its 1_1 inversion doublet (Cheung et al. 1968). Pure rotational transitions of ammonia that arise in the submillimeter region are not observable from the ground, and the fundamental rotational $1_0 \rightarrow 0_0$ transition of NH_3 at 572.5 GHz was first detected by Liseau et al. (2003) and Larsson et al. (2003) with the space submillimeter telescope ODIN toward the low-mass interstellar cloud core ρ Oph A and the Orion bar. Deuterated isotopomers of ammonia are interesting because, due to their higher reduced mass, the rotational levels become closer in energy and cover a lower frequency domain. Consequently, the rotational transitions of these deuterated forms are in a range of frequencies that is not absorbed by the Earth's atmosphere. Mono-deuterated ammonia NH_2D was first observed by Turner et al. (1978) in the molecular cloud Sgr B2 by means of its 1_{11}–1_{01} *ortho* transition at 85.9 GHz. This transition and its associated *para* transition at 110.1 GHz were more recently observed by Tiné et al. (2000) in the dark clouds TMC1 and L134N. Simultaneously, Saito et al. (2000) reported the observations of the *para* transition at 110.1 GHz in several cloud cores. Finally Shah & Wootten (2001) reported a survey of these two lines toward protostellar cores in low-mass star formation regions of the Galaxy.

These observations created a need for collision rate coefficients in order to correctly interpret the different lines and compute kinetic temperature and densities of the molecular component of the ISM via an appropriate treatment of the radiative transfer. Moreover, the future infrared and submillimeter spatial telescope HERSCHEL and the construction of ALMA (Atacama Large Millimeter Array) in Chile increase the need for these detailed molecular data.

The new accurate intermolecular potential energy surface (PES) for NH_3-He of Hodges & Wheatley (2001) has been used to reevaluate the collisional excitation of NH_3 by He (Machin & Roueff 2005). As long as the Born-Oppenheimer approximation can be applied, the same PES can be used for any isotopic substitution of the nuclei because the electrostatic interaction depends only on the relative positions of the electrons and the nuclear charges. However, the center of mass reference frame is modified and the expansion coefficients of the PES over the spherical harmonics, $v_{\lambda\mu}$, are changed accordingly, as shown in Sect. 2. As NH_2D is no longer a symmetric top like NH_3, the formalism of the collision with He is also different and is presented in Sect. 3. The cross sections and the corresponding reaction rate coefficients of the NH_2D-He system are given respectively in Sects. 4 and 5. We present our conclusion in Sect. 6.

2. Potential energy surface

We use the MOLSCAT code version 14 of J. M. Hutson and S. Green to compute the quantal excitation cross sections of NH_2D by He. The electronic potential that describes the interaction between NH_2D and He depends only on the relative positions of electronic and nuclear charges involved in the system. The nuclear charges are the same for any isotopic substitution. Then, the PES describing the NH_3-He system can be used when non adiabatic coupling between electronic and nuclear motion can be neglected (Born-Oppenheimer approximation). We use the recent accurate PES for NH_3-He of Hodges & Wheatley (2001) as in our previous work on NH_3-He (Machin & Roueff 2005).

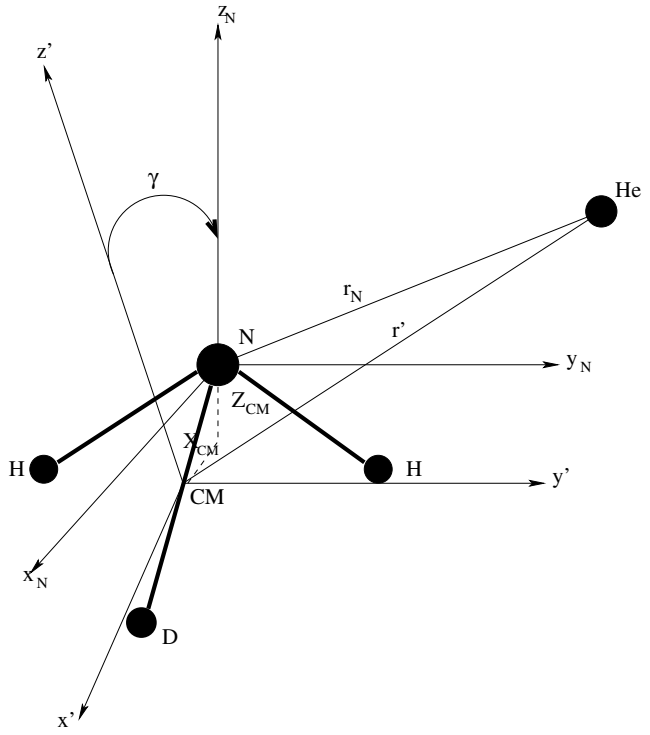

Fig. 1. Relation between the center of mass reference frame (x', y', z') of NH_2D and the reference frame used by Hodges & Wheatley (2001) for their NH_3-He PES (x_N, y_N, z_N). X_{CM} and Z_{CM} are the coordinates of the center of mass of NH_2D in the PES reference frame. γ is the angle between the z_N and the z' axis. CM indicates the center of mass and N the nitrogen atom.

This PES is given in a Cartesian coordinate system (x_N, y_N, z_N) centered on the nitrogen atom, and the z axis is collinear to the axis of symmetry (C_3) of the NH_3 molecule. This axis is perpendicular to the plane of the three hydrogen atoms. However, the collisional equations to be solved in the MOLSCAT program are written in the center of mass system of the molecule (NH_2D) with axes equal to those of the principal inertia momenta noted (x', y', z'). Figure 1 illustrates the relation between the two reference frames.

We express the PES of Hodges & Wheatley (2001) in the MOLSCAT coordinate system. For NH_2D, the transformation is the following:

$$x_N = x' \cos(\gamma) - z' \sin(\gamma) + X_{CM} \quad (1)$$

$$y_N = y' \quad (2)$$

$$z_N = x' \sin(\gamma) + z' \sin(\gamma) + Z_{CM}, \quad (3)$$

where γ is the angle between the z_N and the z' axes and X_{CM} and Z_{CM} are the coordinates of the center of mass of NH_2D in the PES reference frame (x_N, y_N, z_N). The values of γ, X_{CM}, and Z_{CM} are given in Table 1. γ is taken from Cohen & Pickett (1982). X_{CM} and Z_{CM} are calculated for an umbrella angle $\alpha_e = 112.14°$ and for the length of the N-H bond $r_e = 1.9132\ a_0$. These values correspond to the experimental equilibrium geometry given by Benedict et al. (1957) and reported in Hodges & Wheatley (2001). We expand the PES in the body-fixed coordinates as:

$$V(r', \theta', \phi') = \sum_{\lambda\mu} v_{\lambda\mu}(r') Y_{\lambda\mu}(\theta', \phi'). \quad (4)$$

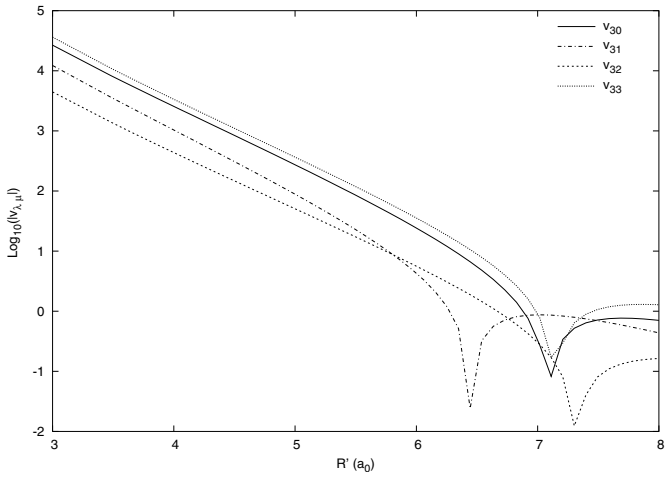

Fig. 2. $v_{\lambda\mu}$ radial coefficients for $\lambda = 3$ of the PES expansion for NH_2D. The decimal logarithms of the absolute value of the coefficients, expressed in reciprocal centimeters, are displayed.

Table 1. Values of γ, X_{CM}, and Z_{CM} for NH_2D in the PES reference frame.

Parameter	NH_2D
γ (in degrees)	–8.57
X_{CM} (a_0)	0.0988
Z_{CM} (a_0)	–0.1611

In the case of NH_3, only $v_{\lambda\mu}(r')$ with $\mu = 3n$ are non-zero due to the C_{3v} symmetry. For NH_2D, this symmetry is broken, so all the $v_{\lambda\mu}(r')$ have to be included. We use the "VRTP" procedure in the MOLSCAT program, which provides the expansion coefficients $v_{\lambda\mu}(r')$ of the PES. Decimal logarithms of the absolute values corresponding to $\lambda = 3$ coefficients are displayed in Fig. 2. The cusps in the figure correspond to a change of sign as the coefficients become negative at large distances. We see that for $v_{3\mu}$ with $\mu = 1$ and $\mu = 2$ coefficients are not negligible compared with the $v_{3\mu}(r')$ with $\mu = 0$ and $\mu = 3$. In the present calculations, we have included $v_{\lambda\mu}(r')$ until $\lambda = 10$, which allows a satisfactory representation of the PES.

3. Collisional treatment

NH_2D is an asymmetric top and is treated as a rigid rotator. The relevant formalism of collisional excitation of asymmetric tops is described in Garrison et al. (1976), Garrison & Lester (1977), and Palma & Green (1987). Two different reference frames are introduced: the body-fixed (BF) frame (x', y', z'), which corresponds to the principal moments of inertia axes system, and the space-fixed (SF) frame (x, y, z), which both have their origin at the center of mass of the molecule. The BF axes are connected to the SF axes by a rotation involving the Euler angles $(\alpha\beta\gamma)$. The rotational Hamiltonian introduced in MOLSCAT is taken as:

$$H_{asymtop} = AJ_{x'}^2 + BJ_{y'}^2 + CJ_{z'}^2 - D_{jj}J^4 - D_{jk}J^2J_{z'}^2 - D_{kk}J_{z'}^4. \quad (5)$$

$J_{x',y',z'}$ represents the components of the rotational angular momentum in the BF reference frame oriented along the principal moments of inertia of the molecule $(I_{x',y',z'})$. The rotational constants are given by $A = \hbar^2/2I_{x'}$, $B = \hbar^2/2I_{y'}$, and $C = \hbar^2/2I_{z'}$, and only the first three distorsion terms are included. The numerical values are displayed in Table 2. The rotational constants are from CDMS (Müller et al. 2001) and the distorsion terms from

Table 2. Values of the rotational constants A, B, and C, and of the centrifugal distortion constants D_{jj}, D_{jk}, and D_{kk} for NH_2D used in this work in units of cm^{-1}.

A	9.6759
B	6.4103
C	4.6968
D_{jj}	5.2772×10^{-4}
D_{jk}	-7.9872×10^{-4}
D_{kk}	3.6537×10^{-4}

Table 3. Energy term values of the rotational levels of NH_2D calculated by MOLSCAT with the rotational and distortion constants of Table 2.

Rotational level	Energy (cm^{-1})
0_{00}	0.0000
1_{01}	11.1062
1_{11}	14.3718
1_{10}	16.0841
2_{02}	32.7961
2_{12}	34.8677
2_{11}	39.9993
2_{21}	49.7961
2_{20}	50.3112
3_{03}	64.2795

Coudert et al. (1986). The derived energy term values of the ten first rotational levels are displayed in Table 3.

To solve the nuclear rotational Schrödinger's equation, it is convenient to expand the asymmetric top wave functions on the symmetric top wave functions.

$$|j\tau m\rangle = \sum_{k=-j}^{j} a_{k\tau}^{j} \, |jkm\rangle, \tag{6}$$

where $|jkm\rangle$ are defined as in Green (1976):

$$|jkm\rangle = \sqrt{\frac{2j+1}{8\pi^2}} \mathcal{D}_{km}^{j}(\alpha\beta\gamma), \tag{7}$$

where j, k, and m are, respectively, the eigenvalues of J^2, $J_{z'}$, and J_z. The $a_{k\tau}^{j}$ are the expansion coefficients that are calculated in the MOLSCAT program for the value ITYPE = 6. τ is an index that labels the asymmetric top rotational states. The ortho and para character of NH_2D levels arises when one takes the overall symmetry of the wavefunction under the exchange of the two protons into account. The result is a removal of the degeneracy without including the inversion operation. However, the corresponding level energies are very close (see, for example, the values summarized in Coudert & Roueff 2006). We do not include the corresponding terms in the Hamiltonian. So, the ortho and para levels are degenerate in our treatment and the corresponding excitation probabilities within the ortho and para symmetry will be identical. In addition, the ortho-para excitation is strictly forbidden. The total Hamiltonian of the system is expressed as:

$$H = -\frac{\hbar^2}{2\mu}\nabla_{\boldsymbol{r}}^2 + H_{\text{asymtop}}(\hat{R}') + V(\boldsymbol{r}, \hat{R}'), \tag{8}$$

where the first term is the kinetic energy operator, the second is the asymmetric top Hamiltonian, and the third the PES. μ is the reduced mass of the system NH_2D-He. The value of μ is taken as 3.2754 amu. $\boldsymbol{r} = (r, \theta, \phi)$ is the position of the helium atom in the SF frame, and $\hat{R}' = (\alpha\beta\gamma)$ is the orientation of the NH_2D molecule in the SF frame. The position of He in the BF frame is given by $\boldsymbol{r}' = (r', \theta', \phi')$ with $r' = r$. Then we have to solve the Schrödinger's equation:

$$H\Psi = E_{\text{tot}}\Psi, \tag{9}$$

where E_{tot} is the total collision energy and Ψ the total eigenfunction that includes the coupling of the rotational angular momentum $\boldsymbol{j}$ and the relative orbital angular momentum $\boldsymbol{\ell}$ of the helium atom to obtain the total angular momentum $\boldsymbol{J} = \boldsymbol{j} + \boldsymbol{\ell}$. Ψ is defined by:

$$\Psi_{j\ell\tau}^{JM}(\boldsymbol{r}, \hat{R}') = \sum_{j'\ell'\tau'} \frac{1}{r} u_{j'\ell'\tau'}^{Jj\ell\tau}(r) |JMj'\ell'\tau'\rangle, \tag{10}$$

$u_{j'\ell'\tau'}^{Jj\ell\tau}(r)$ is the radial part of the wavefunctions, and $|JMj'\ell'\tau'\rangle$ the angular part given by:

$$|JMj\ell\tau\rangle = \sum_{mm_\ell} \langle jm\ell m_\ell | JM\rangle |j\tau m\rangle |\ell m_\ell\rangle. \tag{11}$$

Introducing Eq. (10) in Eq. (8), we have to solve second-order coupled differential equations for the radial part of the wavefunctions:

$$\left[\frac{\mathrm{d}^2}{\mathrm{d}r^2} - \frac{\ell'(\ell'+1)}{r^2} + \kappa_{j'\tau'}^2\right] u_{j'\tau'\ell'}^{Jj\tau\ell}(r) = \frac{2\mu}{\hbar^2} \times \sum_{j''\tau''\ell''} \langle Jj'\tau'\ell' \mid V \mid JMj''\tau''\ell''\rangle u_{j''\tau''\ell''}^{JMj\tau\ell}(r), \tag{12}$$

where $\kappa_{j'\tau'}^2 = \frac{2\mu}{\hbar^2}(E_{\text{tot}} - E_{j'\tau'})$. With the determination of these radial functions and knowing the asymptotic form of these functions, we can define the scattering matrix S^J by:

$$u_{j'\tau'\ell'}^{Jj\tau\ell}(r) \sim \delta_{jj'}\delta_{\tau\tau'}\delta_{\ell\ell'} \exp\left[-\mathrm{i}\left(k_{j\tau}r - \frac{\ell\pi}{2}\right)\right] - \left(\frac{k_{j\tau}}{k_{j'\tau'}}\right)^{\frac{1}{2}} S_{j\tau\ell\to j'\tau'\ell'}^{J} \exp\left[\mathrm{i}\left(k_{j\tau}r - \frac{\ell\pi}{2}\right)\right]. \tag{13}$$

Then the integral cross sections for the transition $j\tau \to j'\tau'$ are given by:

$$\sigma_{j\tau\to j'\tau'} = \frac{\pi}{(2j+1)k_{j\tau}^2} \times \sum_{J=0}^{\infty}(2J+1) \sum_{\ell=|J-j|}^{J+j} \sum_{\ell'=|J-j'|}^{J+j'} |\, T_{j\tau\ell\to j'\tau'\ell'}^{J} \,|^2 \tag{14}$$

with $T_{j\tau\ell\to j'\tau'\ell'}^{J} = \delta_{jj'}\delta_{\tau\tau'}\delta_{\ell\ell'} - S_{j\tau\ell\to j'\tau'\ell'}^{J}$. The detailed balance is verified:

$$\sigma_{j'\tau'\to j\tau} = \frac{(2j+1)k_{j\tau}^2}{(2j'+1)k_{j'\tau}^2}\sigma_{j\tau\to j'\tau'}. \tag{15}$$

This approach, known as the "close-coupling" method can be considered as exact, if one includes all the possible channels (open and closed). In practice one has to limit the number of channels, and it is important to check the convergence of such calculations and include a sufficient number of levels in the expansion. Other collision treatments are implemented in MOLSCAT, such as the coupled-states approximation introduced by McGuire & Kouri (1974). In this approximation,

Table 4. Values of the cross sections (in 10^{-16} cm^2) for some transitions of NH_2D at a total energy of 100 cm^{-1} with an increasing value of the number of rotational states included in the basis. For example B36 indicates a basis of 36 states.

Transition	B36	B49	B64	B81	B100
$0_{00} \rightarrow 1_{01}$	0.6599	0.6565	0.6587	0.6584	0.6583
$0_{00} \rightarrow 1_{10}$	0.9464	0.9375	0.9358	0.9363	0.9361
$0_{00} \rightarrow 2_{02}$	1.0361	1.0366	1.0394	1.0396	1.0397
$1_{01} \rightarrow 0_{00}$	0.2474	0.2462	0.2470	0.2469	0.2469
$1_{01} \rightarrow 1_{11}$	0.4594	0.4619	0.4608	0.4615	0.4614
$1_{01} \rightarrow 1_{10}$	0.4310	0.4365	0.4392	0.4394	0.4395
$1_{01} \rightarrow 2_{02}$	3.6718	3.6777	3.6859	3.6889	3.6891
$1_{11} \rightarrow 1_{01}$	0.4770	0.4795	0.4783	0.4791	0.4790
$1_{11} \rightarrow 1_{10}$	0.2954	0.2906	0.2902	0.2899	0.2899
$1_{11} \rightarrow 2_{02}$	0.4333	0.4314	0.4401	0.4405	0.4406

scattering equations are written in the BF frame, which is rotating. Then the projection of the orbital angular momentum is restricted to the value $m_\ell = 0$. This method gives satisfactory results as shown in Machin & Roueff (2005) for the NH_3-He system and is much less expensive in CPU time. As the reduced mass of NH_2D is larger than the reduced mass of NH_3, more energy levels than in the NH_3-He case have to be included for a given total collision energy. We used the coupled states approximation for data production after checking the validity of the approximation at some specific energies. The resulting uncertainty should not exceed a few percent on the computed collision rates.

4. Calculations of the cross sections

We carefully checked the convergence of the S matrix for different collision parameters defined in MOLSCAT. The size of the basis set in the PES expansion, i.e., the number of $v_{\lambda\mu}$ included in the calculations has been chosen to be 45 and includes terms up to $\lambda = 8$ for energies up to 100 cm^{-1}. At higher energies, 66 expansion coefficients have been introduced and include terms up to $\lambda = 10$. To illustrate this point we display some convergence tests for a total collision energy of 100 cm^{-1} in Tables 4 and 5. On the other hand, 100 (144) rotational states have been included in the basis function for an energy of 100 (400) cm^{-1} corresponding to a maximum energy of 830 (1224) cm^{-1}.

We display the chosen input parameters used in MOLSCAT in Table 6. JTOTU = –1 means that MOLSCAT is checking itself for the convergence regarding the maximum J taken into account. Calculations have been performed for a total energy range between 11.1 cm^{-1} and 400 cm^{-1}. The energy step has been varied with increasing collision energy. It is 0.1 cm^{-1} for a total energy range between 11.1 cm^{-1} and 100 cm^{-1}, 1 cm^{-1} between 100 cm^{-1} and 340 cm^{-1}, and 5 cm^{-1} between 340 cm^{-1} and 400 cm^{-1}.

Figure 3 illustrates the dependence of the $1_{11} \rightarrow 1_{01}$ cross section as a function of the relative kinetic energy between NH_2D and He. This transition at 85 GHz was first detected by Turner et al. (1978). A resonance structure is found at low energies. The peaks are due to the opening of new collision channels and correspond to so-called Feshbach resonances. Figure 4 displays a zoom of Fig. 3 in the energy range between 0 and 120 wavenumbers where the resonances appear. A small energy step is required in the calculations to fully account for the energy dependence of the cross sections that may affect the results for the rate coefficients at very low temperatures.

Table 5. Values of the cross sections (in 10^{-16} cm^2) for some transitions of NH_2D at a total energy of 100 cm^{-1} with an increasing value of the number of radial coefficients $v_{\lambda\mu}$ included in the expansion of the PES. For example L45 means that 45 $v_{\lambda\mu}$ were taken into account in the expansion.

Transition	L28	L45	L55
$0_{00} \rightarrow 1_{01}$	0.6545	0.6583	0.6580
$0_{00} \rightarrow 1_{10}$	0.9298	0.9361	0.9365
$0_{00} \rightarrow 2_{02}$	1.0392	1.0397	1.0396
$1_{01} \rightarrow 0_{00}$	0.2454	0.2469	0.2467
$1_{01} \rightarrow 1_{11}$	0.4581	0.4614	0.4616
$1_{01} \rightarrow 1_{10}$	0.4390	0.4395	0.4395
$1_{01} \rightarrow 2_{02}$	3.6837	3.6892	3.6928
$1_{11} \rightarrow 1_{01}$	0.4756	0.4790	0.4792
$1_{11} \rightarrow 1_{10}$	0.2883	0.2899	0.2897
$1_{11} \rightarrow 2_{02}$	0.4403	0.4406	0.4405

Table 6. Values of input parameters of MOLSCAT using in our calculations.

Parameter	Value
RMIN	3.0
INTFLG	6
STEPS	10.0
JTOTU	–1
NPTS	14, 14

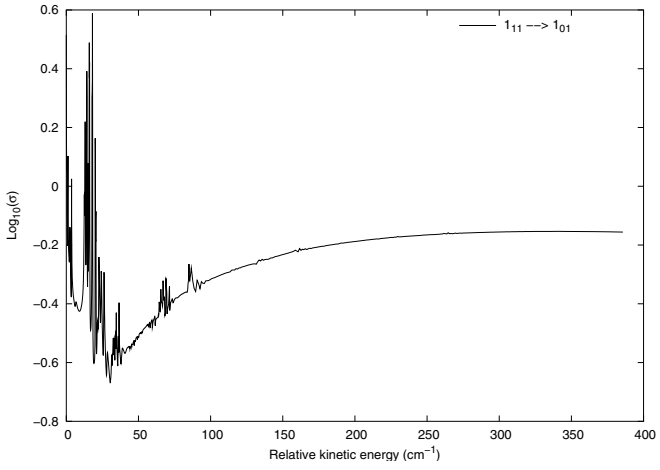

Fig. 3. Decimal logarithm of the cross section σ (in 10^{-16} cm^2) as a function of the relative kinetic energy for the transition $1_{11} \rightarrow 1_{01}$ of NH_2D.

5. Rate coefficients for NH_2D-He

The collisional (de)excitation rate coefficients in function of the temperature T are obtained via a Maxwellian average of the

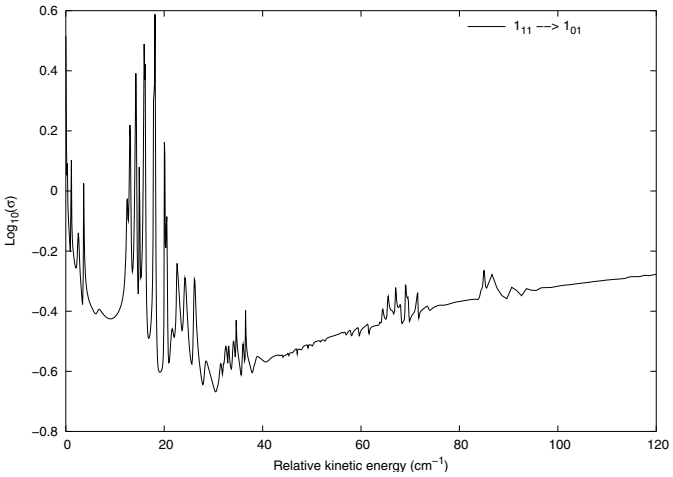

Fig. 4. Resonance structure in the cross section σ of the $1_{11} \rightarrow 1_{01}$ transition. Decimal logarithm of σ (in 10^{-16} cm^2) in function of the relative kinetic energy of NH_2D and He.

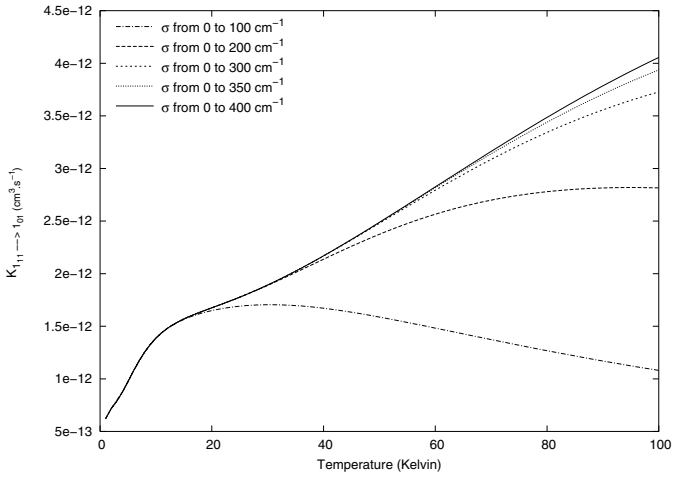

Fig. 5. Rate coefficients $K_{1_{11} \rightarrow 1_{01}}$ (cm^3 s^{-1}) of the transition $1_{11} \rightarrow 1_{01}$ in function of the temperature obtained for different values of the maximum total energy in the integration performed in Eq. (16): 100 cm^{-1}, 200 cm^{-1}, 300 cm^{-1}, 350 cm^{-1}, and 400 cm^{-1}.

cross sections times relative velocity. The integration formula is recalled below:

$$K_{j\tau \rightarrow j'\tau'}(T) = \left(\frac{8k_{\rm B}T}{\pi\mu}\right)^{\frac{1}{2}} \left(\frac{1}{k_{\rm B}T}\right)^2 \times \int_o^\infty \sigma_{j\tau \rightarrow j'\tau'}(E_{\rm tot})\, E\, \exp\left(-\frac{E}{k_{\rm B}T}\right) {\rm d}E, \qquad (16)$$

where E is the relative kinetic energy, $k_{\rm B}$ is the Boltzmann constant, and μ is the reduced mass of the NH_2D-He system. As the integration should be performed until an infinite value of the relative kinetic energy, actual calculations introduce a maximum value that should be significantly larger than the mean thermal energy given approximately by $k_{\rm B}T$, where the decreasing exponential brings a negligible contribution. As cross sections have only been computed until 400 cm^{-1}, we have calculated the rate coefficients for temperatures between 5 K and 100 K that are relevant for the interstellar medium. We show the effect of the energy cut-off on the computed rate coefficients in Fig. 5. In this figure, we see that the rate coefficients of the $1_{11} \rightarrow 1_{01}$ transition are identical for temperatures between 5 and 20 K, whatever value is used for the energy cut-off. However, the situation is somewhat different for higher temperatures where the values obtained for the rate coefficients are quite different for a low value of the cut-off. We estimate that the convergence is attained at 100 K when we integrate Eq. (16) until E = 400 cm^{-1}, as the differences between the rate coefficients become quite close for maximum energy values of 300, 350, and 400 cm^{-1}. We estimate that the resulting error is of the order of 3%.

We have also checked the detailed balance via independent integrations of the excitation and de-excitation cross-sections to validate our results. The detailed balance conditions on the rate coefficients are then verified with an error that does not exceed 1% at the lower temperatures and 0.1% at the higher temperatures. We display the values of the rate coefficients corresponding to transitions of NH_2D induced by He collisions, involving the lowest energy levels for temperatures between 5 and 100 K in Table 7. The temperature variation is smooth, as one can see from the values displayed in Table 7, and collisional de-excitation rate coefficients slightly increase with temperature.

Molecular hydrogen is the main constituent of interstellar molecular clouds and the interpretation of astrophysical spectra requires knowledge of collision rates of molecules with molecular hydrogen. Helium is often considered as a prototype of molecular hydrogen in its para form, $j = 0$, which is probably the most abundant populated level in cold dark interstellar clouds. Then, rate coefficients for NH_2D-para-H_2 can be tentatively deduced from those involving He, if one assumes that the collision probabilities are identical. The values of the rate coefficients of NH_2D-H_2 may then be estimated as the product of the rate coefficients for NH_2D-He by the square root of the ratio of the reduced masses (here 1.3441).

Astrophysicists define a critical density corresponding to a specific transition as the ratio between the Einstein coefficients A_{if} and the rate coefficients K_{if} for a specific collider. This value sets the limit of the perturber density above which the transitions are thermalized. Table 8 displays the estimated values of the critical densities of H_2 thus derived for some specific transitions. We see that the critical density corresponding to the 85 GHz transition ($1_{10} \rightarrow 1_{11}$) is of the order of 2×10^4 cm^{-3}, whereas those corresponding to higher frequency transitions involving the ground rotational level attain values larger than 10^6 cm^{-3}.

6. Conclusions

Rotational excitation cross sections of NH_2D induced by He collisions are presented for the first time. Calculations have been performed in the quantal CS approximation by including the couplings arising from the change of the reference frame from the NH_3-He system. The total collision energy range is extending from 11.1 cm^{-1} to 400 cm^{-1}. Collision rate coefficients have been derived for temperatures relevant to interstellar conditions, from 5 K to 100 K. Deuteration fractionation processes may take place in low temperature conditions where deuterated isotopologs are detected. The values of the rate coefficients are available on request to the authors and will be part of the Basecol database[1]. Similar computations are performed for ND_2H perturbed by He. These values may also be used as a first guess to derive NH_2D rotational excitation due to para-H_2 in astrophysical applications by using the weighting factor 1.3441 deduced from reduced mass effects. Calculations involving the appropriate PES are under way.

[1] Basecol, `http://amdpo.obspm.fr/basecol`

Table 7. Einstein coefficients and rate coefficients for NH_2D-He for different temperatures. Only de-excitation transitions are considered. Numbers in parentheses correspond to the power of ten. Einstein coefficients are taken from the CDMS database (Müller et al. 2001) and are given for the *ortho* and *para* transitions.

Transition	Einstein coefficients A_{if} (s^{-1})		Rate coefficients K_{if} ($cm^3\ s^{-1}$)					
	ortho	*para*	5 K	10 K	25 K	50 K	75 K	100 K
$1_{01} \rightarrow 0_{00}$	7.82(–6)	7.29(–6)	7.56(–13)	7.75(–13)	1.04(–12)	1.41(–12)	1.70(–12)	1.90(–12)
$1_{11} \rightarrow 1_{01}$	7.82(–6)	1.65(–5)	9.74(–13)	1.39(–12)	1.78(–12)	2.49(–12)	3.33(–12)	4.06(–12)
$1_{10} \rightarrow 0_{00}$	8.55(–4)	9.95(–4)	9.56(–13)	9.83(–13)	1.29(–12)	1.94(–12)	2.58(–12)	3.09(–12)
$1_{10} \rightarrow 1_{01}$	–	–	4.47(–12)	3.95(–12)	3.50(–12)	3.48(–12)	3.60(–12)	3.72(–12)
$1_{10} \rightarrow 1_{11}$	4.36(–8)	4.05(–8)	1.42(–12)	1.41(–12)	1.48(–12)	1.82(–12)	2.16(–12)	2.43(–12)
$2_{02} \rightarrow 0_{00}$	–	–	2.42(–12)	2.34(–12)	2.17(–12)	2.23(–12)	2.39(–12)	2.52(–12)
$2_{02} \rightarrow 1_{01}$	–	–	1.51(–11)	1.51(–11)	1.61(–11)	1.92(–11)	2.18(–11)	2.36(–11)
$2_{02} \rightarrow 1_{11}$	–	–	2.45(–12)	2.37(–12)	2.28(–12)	2.34(–12)	2.46(–12)	2.56(–12)
$2_{02} \rightarrow 1_{10}$	1.57(–4)	1.35(–4)	2.72(–13)	3.21(–13)	3.31(–13)	3.60(–13)	4.26(–13)	4.89(–13)
$2_{12} \rightarrow 1_{01}$	–	–	1.22(–12)	1.11(–12)	9.63(–13)	9.67(–13)	1.03(–12)	1.10(–12)
$2_{12} \rightarrow 1_{11}$	–	–	1.51(–11)	1.39(–11)	1.41(–11)	1.68(–11)	1.93(–11)	2.11(–11)
$2_{12} \rightarrow 1_{10}$	–	–	4.68(–14)	7.87(–14)	1.48(–13)	2.40(–13)	3.81(–13)	5.26(–13)
$2_{12} \rightarrow 2_{02}$	1.81(–6)	5.92(–6)	1.38(–12)	1.51(–12)	2.06(–12)	3.07(–12)	4.09(–12)	4.92(–12)
$2_{11} \rightarrow 0_{00}$	–	–	1.02(–12)	1.01(–12)	1.06(–12)	1.25(–12)	1.46(–12)	1.63(–12)
$2_{11} \rightarrow 1_{01}$	4.62(–3)	5.02(–3)	1.58(–12)	1.57(–12)	1.79(–12)	2.39(–12)	2.97(–12)	3.43(–12)
$2_{11} \rightarrow 1_{11}$	–	–	3.50(–11)	3.57(–11)	3.64(–11)	3.83(–11)	3.95(–11)	3.98(–11)
$2_{11} \rightarrow 1_{10}$	6.49(–5)	7.07(–5)	1.07(–12)	1.08(–12)	1.29(–12)	1.80(–12)	2.30(–12)	2.68(–12)
$2_{11} \rightarrow 2_{02}$	–	–	3.01(–12)	2.82(–12)	2.31(–12)	2.23(–12)	2.38(–12)	2.56(–12)
$2_{11} \rightarrow 2_{12}$	4.16(–7)	6.42(–7)	4.48(–12)	5.28(–12)	8.09(–12)	1.21(–11)	1.52(–11)	1.74(–11)
$2_{21} \rightarrow 1_{01}$	–	–	2.59(–11)	2.65(–11)	2.78(–11)	3.01(–11)	3.18(–11)	3.27(–11)
$2_{21} \rightarrow 1_{11}$	–	–	2.89(–12)	2.85(–12)	3.09(–12)	3.69(–12)	4.29(–12)	4.73(–12)
$2_{21} \rightarrow 1_{10}$	–	–	8.32(–13)	8.46(–13)	8.48(–13)	9.09(–13)	9.85(–13)	1.05(–12)
$2_{21} \rightarrow 2_{02}$	–	–	4.96(–12)	5.23(–12)	6.35(–12)	8.25(–12)	9.85(–12)	1.10(–11)
$2_{21} \rightarrow 2_{12}$	–	–	3.57(–12)	3.54(–12)	3.60(–12)	4.14(–12)	4.89(–12)	5.55(–12)
$2_{21} \rightarrow 2_{11}$	1.18(–4)	9.22(–5)	1.20(–12)	1.30(–12)	1.59(–12)	2.13(–12)	2.66(–12)	3.06(–12)
$2_{20} \rightarrow 0_{00}$	–	–	9.52(–12)	9.51(–12)	1.01(–11)	1.17(–11)	1.30(–11)	1.38(–11)
$2_{20} \rightarrow 1_{01}$	–	–	9.54(–13)	1.00(–12)	1.24(–12)	1.61(–12)	1.91(–12)	2.12(–12)
$2_{20} \rightarrow 1_{11}$	–	–	1.06(–12)	1.09(–12)	1.19(–12)	1.35(–12)	1.50(–12)	1.60(–12)
$2_{20} \rightarrow 1_{10}$	–	–	3.38(–12)	3.30(–12)	3.51(–12)	4.28(–12)	5.04(–12)	5.61(–12)
$2_{20} \rightarrow 2_{02}$	–	–	2.18(–11)	2.13(–11)	1.97(–11)	1.90(–11)	1.89(–11)	1.87(–11)
$2_{20} \rightarrow 2_{12}$	2.09(–4)	1.79(–4)	9.86(–13)	1.01(–12)	9.74(–13)	1.10(–12)	1.27(–12)	1.41(–12)
$2_{20} \rightarrow 2_{11}$	–	–	2.68(–12)	2.67(–12)	2.66(–12)	2.93(–12)	3.33(–12)	3.68(–12)
$2_{20} \rightarrow 2_{21}$	1.46(–9)	1.52(–9)	2.42(–12)	2.42(–12)	2.44(–12)	2.97(–12)	3.62(–12)	4.15(–12)

Table 8. Critical density for some *ortho* and *para* transitions of NH_2D with H_2. Collision rate coefficients for NH_2D-H_2 are those for NH_2D-He multiplied by the reduced masses ratio of 1.3441. Densities are in cm^{-3}.

Transition	Critical density (cm^{-3})	
	ortho	*para*
$1_{01} \rightarrow 0_{00}$	7.51×10^6	7.00×10^6
$1_{11} \rightarrow 1_{01}$	4.19×10^6	8.85×10^6
$1_{10} \rightarrow 0_{00}$	6.47×10^8	7.51×10^8
$1_{10} \rightarrow 1_{11}$	2.30×10^4	2.14×10^4
$2_{02} \rightarrow 1_{10}$	3.64×10^8	3.13×10^8
$2_{12} \rightarrow 2_{02}$	8.93×10^5	2.92×10^6
$2_{11} \rightarrow 1_{01}$	2.19×10^9	2.38×10^9
$2_{11} \rightarrow 1_{10}$	4.47×10^7	4.87×10^7
$2_{11} \rightarrow 2_{12}$	5.86×10^4	9.08×10^4
$2_{21} \rightarrow 2_{11}$	6.76×10^7	5.27×10^7
$2_{20} \rightarrow 2_{12}$	1.54×10^8	1.32×10^8
$2_{20} \rightarrow 2_{21}$	4.48×10^2	4.67×10^2

Acknowledgements. We are grateful to Marie-Lise Dubernet of LERMA-Meudon and Pierre Valiron of the Laboratoire d'Astrophysique de Grenoble for useful discussions. This work is one of the tasks defined in the European FP6 network "The Molecular Universe".

References

Benedict, W. S., Gailar, N., & Plyler, E. K. 1957, Can. J. Phys., 35, 1235
Cheung, A. C., Rank, D. M., Townes, C. H., Thornton, D. D., & Welch, W. J. 1968, Phys. Rev. Lett., 21, 1701
Cohen, A. E., & Pickett, H. M. 1982, J. Mol. Spectrosc., 93, 83
Coudert, L., & Roueff, E. 2006, Astron. & Astrophys., 449, 855
Coudert, L., Valentin, A., & Henry, L. 1986, J. Mol. Spectrosc., 120, 185
Garrison, B. J., Lester, W. A., & Miller, W. H. 1976, J. Chem. Phys., 65, 2193
Garrison, B. J., & Lester, W. A. 1977, J. Chem. Phys., 66, 531
Green, S. 1976, J. Chem. Phys., 64, 3463
Hodges, M. P., & Wheatley, R. J. 2001, J. Chem. Phys., 114, 8836
Larsson, B., Liseau, R., Bergman, P., et al. 2003, A&A, 402, L69
Liseau, R., Larsson, B., Brandeker, A., et al. 2003, A&A, 402, L73
Machin, L., & Roueff, E. 2005, J. Phys. B: At. Mol. Opt. Phys., 38, 1519
McGuire, P., & Kouri, D. J. 1974, J. Chem. Phys., 60, 2488
Hutson, J. M., & Green, S. 1995, MOLSCAT computer code, version 14, distibuted by collaborative computational project No. 6 of the Science and Engineering Research Council, UK
Müller, H. S. P., Thorwirth, S., Roth, D. A., & Winnewisser, G. 2001, A&A, 370, L49
Palma, A., & Green, S. 1987, ApJ, 316, 83
Saito, S., Ozeki, H., Ohishi, M., & Yamamoto, S. 2000 ApJ, 535, 227
Shah, R. Y., & Wootten, A. 2001, ApJ, 554, 933
Tiné, S., Roueff, E., Falgarone, E., Gerin, M., & Pineau des Forêts, G. 2000, A&A, 356, 1039
Townes, C. H., & Schawlow, A. L. 1975, Microwave Spectroscopy (New York: Dover Publications)
Turner, B. E., Zuckerman, B., Morris, M., & Palmer, P. 1978, ApJ, 219, L43